Kinetics and Thermodynamics of Triple-Helix Formation: Effects of Ionic Strength and Mismatches

M. Rougée,* B. Faucon, J. L. Mergny, F. Barcelo,‡ C. Giovannangeli, T. Garestier, and C. Hélène

Laboratoire de Biophysique, Muséum National d'Histoire Naturelle, INSERM U201, CNRS UA481, 43 rue Cuvier, 75005 Paris, France

Received February 4, 1992; Revised Manuscript Received May 20, 1992

ABSTRACT: Thermodynamic and kinetic parameters for the triplex-forming reactions between a homopurine–homopyrimidine 22-base-pair duplex (sequence of the purine strand: 5′d[AAAGGAGGAGAAGAA-GAAAAAA]3′) and the four 22-dN third strands (22 dN: 5′d[TTTCCTCCTCT*N*CTTCTTTTTT]3′, where N = A, C, T, or G) were determined from thermal denaturation and renaturation UV absorbance profiles. Cooling and heating curves were not superimposable and thus allowed us to determine the rate constants of association (k_{on}) and dissociation (k_{off}) as a function of temperature, assuming a two-state model analogous to that developed for duplex-forming reactions. Experiments were performed in 10 mM cacodylate buffer (pH 6.8) in the presence of NaCl concentrations ranging from 20 to 300 mM. Within experimental accuracy, the main results are the following: (i) The rate constants k_{on} and k_{off} result in linear Arrhenius plots, consistent with the prediction of two-state association and dissociation. (ii) k_{on} is independent of the nature of the base N located in the center of the third strand. (iii) k_{on} strongly decreases when the NaCl concentration is decreased. (iv) The activation energy, E_{on}, is always negative and becomes more negative when the NaCl concentration is decreased. (v) k_{off} is independent of NaCl concentration but depends on the base N, with its magnitude following the order C > G > A ≫ T. (vi) The activation energy, E_{off}, is independent of the base N. All these results are discussed in the light of a nucleation-zipping model similar to that developed for the duplex–coil transitions [Craig, M. E., Crothers, D. M., & Doty, P. (1971) J. Mol. Biol. *62*, 383–401; Pörschke, D., Eigen, M. (1971) J. Mol. Biol. *62*, 361–381].

Triple-stranded nucleic acid structures containing one strand of poly(rA) and two strands of poly(rU) were described for the first time more than 30 years ago (Felsenfeld, et al., 1957). Several years later, DNA–DNA–RNA triplexes (Morgan & Wells, 1968) and triplexes containing one strand of poly(dG) and two strands of poly(dC) (Marck & Thiele, 1978) were reported. It has been shown more recently that local triple-helix structures can be obtained by targeting a homopyrimidine oligodeoxynucleotide to a homopurine–homopyrimidine tract of double-helical DNA (Le Doan et al., 1987, Moser & Dervan, 1987, Lyamichev et al., 1988). Recognition of the sequence is achieved through Hoogsteen hydrogen bonding of thymine and protonated cytosine with A·T and G·C Watson–Crick base pairs, respectively (de los Santos et al., 1989; Rajagopal & Feigon, 1989; Pilch et al., 1990b), and does not require denaturation of the double-stranded helix. In these intermolecular triplexes, the homopyrimidine oligodeoxynucleotide strand is located in the major groove of the underlying duplex, in a parallel orientation with respect to the homopurine strand of the duplex.

Formation of the triple helix results in a hypochromism in the UV absorption band located near 260 nm. Hence, thermally induced association and dissociation can be monitored at this wavelength by absorbance versus temperature profiles (Sun et al., 1989). Standard molar thermodynamic parameters ($\Delta H°$, $\Delta S°$) related to formation of the triple helix from the duplex and third strand may be obtained from these profiles, in a manner anologous to that used for the duplex–coil transitions of oligodeoxynucleotides, with the same assumptions and limitations.

Recording an absorbance versus temperature curve while continuously increasing (heating or dissociation curve) or decreasing (cooling or association curve) the temperature of a sample is a dynamic process. Thus, a prerequisite for the recovery of thermodynamic, i.e., equilibrium, parameters from these curves is that they are truly equilibrium curves. This condition dictates that the sample must be heated or cooled at a much slower rate than that of the association–dissociation reaction under study. A simple and useful criterion for this is the coincidence of the heating and cooling curves at the chosen rate of heating and cooling. Heating and cooling rates, of up to 0.5 °C min^{-1}, are generally slow enough to ensure attainment of equilibrium in the cases of duplex–coil transitions in oligodeoxynucleotides. A typical value of 10^6 M^{-1} s^{-1} for the association rate constant results in an association lifetime on the order of seconds for micromolar DNA concentrations; the dissociation lifetime, which is DNA concentration independent, is of the same order of magnitude within the temperature range of the transition.

In contrast, the rate of triplex-forming reactions can be very slow at micromolar concentrations of DNA and depends on the ionic strength and pH in the case of oligodeoxypyrimidine containing cytosines. Early experiments on poly(rA)·2poly(rU) (Blake & Fresco, 1966; Blake et al., 1967, 1968) and oligo(rA)·2oligo(rU) (Pörschke & Eigen, 1971) showed that the association–dissociation rates of triple helices are 100 or more times slower than those of double helices, (Pörschke & Eigen, 1971; Blake & Fresco, 1966; Blake et al., 1967, 1968). Recently, using an *Ava*I restriction endonuclease assay, Maher et al. (1990) determined the second-order rate constant (k_{assn}) for the binding of a 21-nucleotide-long oligopyrimidine containing 5-methylcytosines to a 21-bp duplex in a 6.4-kbp plasmid, as well as the first-order rate constant for the dissociation (k_{diss}) of the triple helix.

* Author to whom correspondence should be addressed.
‡ Permanent address: Universitat de les Illes Balears, Dpto. de Biologia i Ciències de la Salut, Palma de Mallorca, Spain.

0006-2960/92/0431-9269$03.00/0

22dR : 5'd(A A A G G A G G A G A A G A A G A A A A A A)3'

22dY : 3'd(T T T C C T C C T C T T C T T C T T T T T T)5'

22dN : 5'd(T T T C C T C C T C T **N** C T T C T T T T T T)3'

(N = A, T, C or G)

FIGURE 1: Oligodeoxynucleotides used in this study. The homopurine and homopyrimidine strands of the duplex are called 22 dR and 22 dY, respectively. Formation of a triplex has been investigated with a fully complementary (in terms of Hoogsteen base pairing) third strand (22 dT) or a mismatched one (22 dC, 22dG, and 22 dA, corresponding to N = C, G, and A, respectively).

Depending on the reaction conditions, k_{assn} ranged from 8×10^2 to 2.2×10^3 M^{-1} s^{-1}, which was approximately 10^3 times lower than the corresponding value for duplex formation, and k_{diss} ranged from 2.2×10^{-5} to 2.4×10^{-4} s^{-1}, resulting in triplex lifetimes ranging from about 1 h to more than 10 h at 37 °C.

We have ourselves observed in many cases that the thermal dissociation (heating) curves of triple helices of similar length (15–25 triplets) are largely shifted toward higher temperatures with respect to the association (cooling) curves, even at moderate ionic strength (0.1 M NaCl). Preliminary experiments on the system presented in Figure 1, in 10 mM cacodylate and 0.1 M NaCl, showed that hysteresis and triplex stability are strongly dependent on pH within the range 5.8–7.2. At pH 5.8, the heating and cooling curves are superimposed and the corresponding triplex–duplex transitions tend to merge with the dissociation of the duplex into single strands. At pH 7.2, the triplex is destabilized and the association is exceedingly slow and not complete at 0 °C. At pH 6.8, the triplex–duplex transition is well separated from the duplex dissociation with a range of about 10 °C between the end of the triplex–duplex transition and the beginning of the duplex dissociation and the triplex is fully formed above 0 °C. These observations prompted us to study in some detail the kinetic behavior of the system described in Figure 1 at pH 6.8, in order to obtain the rate constants of association and dissociation from the hysteresis of the thermally induced association–dissociation reactions.

In Figure 1 the sequences of the six 22-mer oligodeoxyribonucleotides used in this study are presented. 22 dR and 22 dY are two complementary homopurine and homopyrimidine strands, respectively, which interact to form a duplex via Watson–Crick hydrogen bonding. The four 22-dN strands (N = A, T, C, G) were chosen to interact with this duplex by means of Hoogsteen base pairing to form the T×A·T and C^+×G·C base triplets. The orientation of the 22-dN third strand is parallel to the purine strand of the duplex. For N = A, C, or G, a single mismatch is introduced in the center of the triplex in order to determine its influence on the kinetics and the thermodynamics of the association–dissociation reaction.

MATERIALS AND METHODS

Oligodeoxyribonucleotides were synthesized on a Pharmacia automatic DNA synthesizer by phosphoramidite chemistry and were purified by HPLC. All concentrations are given on a per strand basis and were determined spectrophotometrically using the following molar extinction coefficients at 260 nm calculated from a nearest-neighbor model (Cantor & Warshaw, 1970): 22 dR, $\epsilon = 2.60 \times 10^5$ M^{-1} cm^{-1}; 22 dY, $\epsilon = 1.72 \times 10^5$ M^{-1} cm^{-1}; 22 dA, $\epsilon = 1.77 \times 10^5$ M^{-1} cm^{-1}; 22 dG, $\epsilon = 1.73 \times 10^5$ M^{-1} cm^{-1}; 22 dC = 22 dT, $\epsilon = 1.72 \times 10^5$ M^{-1} cm^{-1}. All experiments were carried out in 10 mM cacodylate buffer (pH 6.8) in the presence of various NaCl concentrations ranging from 20 to 300 mM. Some experiments were performed in the presence of $MgCl_2$.

Preparation of Solutions. A stock concentrated aqueous solution of the target duplex 22 dR·22 dY was used throughout our study. It was prepared by mixing aqueous solutions of the separated strands in a 1/1 molar ratio at room temperature, heating the mixture at 85 °C, and then cooling it slowly (at 1.0×10^{-3} K s^{-1}) to 4 °C with storage at that temperature. Stock concentrated aqueous solutions of the four 22-dN strands were also prepared and stored in the same manner. Working solutions of the duplex plus the third 22-dN strand in a 1/1 duplex/22 dN molar ratio were prepared by mixing appropriate amounts of the stock solutions and adding buffer and NaCl to give the final solution at the appropriate concentration in strands, buffer, and NaCl. The solutions were vortexed, introduced into quartz optical cells, and overlaid with a thin layer of paraffin oil to prevent evaporation. The cells were weighed before and after each experiment to check for evaporation. The optical path lengths were 1 and 0.2 cm for 1 and 5 μM strand concentrations, respectively.

UV Absorption Spectrophotometry. Absorbance versus temperature heating and cooling curves were obtained using a Kontron-Uvikon 820 spectrophotometer. The temperature of the six-cell holder was regulated by a circulating liquid (80% water–20% glycerol) using a Haake cryothermostat and monitored by a thermoresistor immersed in an accompanying cell containing only buffer. Constant heating or cooling rates, dT/dt, were obtained using a Haake PG20 temperature programmer. The rates of temperature changes ranged from $\pm 1.5 \times 10^{-4}$ to $\pm 8.0 \times 10^{-3}$ K s^{-1}. Absorbance and temperature were recorded at appropriate constant time intervals, depending on the conditions, in order to record one absorbance value per degree. In separate experiments, control of the response time of the thermoresistor was conducted by recording the heating and cooling profiles of selected mixtures of poly(rA) and $d(T)_8$ in a medium of low ionic strength (35 mM NaCl) such that the corresponding helix–coil transitions occurred in the temperature range spanned in our study (typically 0–40 °C). For this fast system, cooling and heating profiles were superimposable, except at the highest rates ($>5 \times 10^{-3}$ K s^{-1}), where the heating curve was shifted toward lower temperatures by a few tenths of a degree. This shift was largely negligible with respect to the width of the hysteresis of the triple-helix system, recorded simultaneously.

Spectrophotometric stability during the long times of most of the experiments was systematically checked by simultaneously recording the absorbance of an accompanying cell containing the target duplex. The absorbance ($A \sim 0.35$) of the duplex between 0 and 40 °C, where the triplex-forming samples have an absorbance varying typically between 0.5 and 0.6, was routinely observed to be constant within ±0.001. Water condensation on the cell walls at low temperatures was prevented by gently blowing a stream of dry air into the cell compartment.

Description of a Typical Experiment. The working solution containing the duplex plus the 22-dN strand in a 1/1 molar ratio was first heated to a few degrees below the onset of dissociation of the duplex and maintained at that temperature until a constant absorbance reading was achieved. In all cases, the temperature of the sample was never allowed to exceed this temperature, which constitutes a reference for complete separation of the third strand from the duplex without duplex dissociation. The solution was then cooled at an appropriate constant rate $-dT/dt$ to about 0 °C and maintained at that temperature until the absorbance reading was constant. The time needed to reach this low-temperature equilibrium state was strongly dependent on the cooling rate $-dT/dt$ and on the intrinsic rate of association of the third strand to the duplex and reached hours in some cases. The solution was then heated at an appropriate constant rate (generally the same as the cooling rate, $+dT/dt$) to the starting temperature. From this first cycle, the rate constants for the association and dissociation reactions were deduced as explained below. In subsequent experiments on the same solution, several heating and cooling curves were recorded, varying the rates of temperature changes ($\pm dT/dt$). In some cases, either the temperature was held constant to monitor isothermal absorbance changes or the direction of temperature change was reversed at some selected temperature without waiting for attainment of equilibrium. Finally, the sample was heated to the starting temperature to ensure that the initial absorbance was unchanged. All these experiments were performed in order to check the validity of the model used to describe the association–dissociation reaction.

Data Analysis. Our data have been analyzed within the framework of a concerted "two-state" or "all-or-none" model of association–dissociation, such as that developed for the double-helix to coil transitions of complementary oligonucleotides. The main argument in favor of this simple model comes from kinetic data, i.e., from the observation that the reaction between complementary single-stranded oligonucleotides giving the duplex helix can be adequately described by a second-order association as opposed to a first-order dissociation reaction. In this model, it is assumed that species with incomplete base pairing are not significantly populated, so that the only absorbing species are the separated strands and the fully formed duplex. Justifications and limitations of this model have been presented and discussed in many theoretical and experimental papers (Craig et al., 1971; Pörschke & Eigen, 1971; Anshelevich et al., 1984) and classical textbooks (Cantor & Schimmel, 1980). In the case of a triplex-forming reaction from a duplex and a third oligopyrimidine strand, the reaction may be symbolized by

$$D + M \underset{k^T_{off}}{\overset{k^T_{on}}{\rightleftharpoons}} Tr \quad (K^T_{eq} = k^T_{on}/k^T_{off}) \qquad (1)$$

The rate equation associated with this reaction is

$$d[D]/dt = d[M]/dt = -d[Tr]/dt = -k^T_{on}[D][M] + k^T_{off}[Tr] \qquad (2)$$

where D, M, and Tr are the duplex, the third strand, and the triplex, respectively, and the brackets indicate concentrations.

Under our conditions, D and M are added in an equimolar ratio, but in experiments where the probing third strand M is targeted to a duplex D, this is generally not the case, and usually, [M] > [D]. In order to focus on this latter point, let us define

$$D_T = [D] + [Tr] \qquad M_T = [M] + [Tr]$$

$\alpha = [Tr]/D_T$, where α is the fraction of the duplex engaged in the triplex $0 \leq \alpha \leq 1$. D being the species (duplex) with the lowest concentration, $\rho = M_T/D_T \geq 1$.

The rate eq 2 is easily transformed into

$$d\alpha/dt = k^T_{on} M_T (1 - \alpha)(1 - \alpha/\rho) - k^T_{off}\,\alpha \qquad (3)$$

The extent of association α is related to the absorbance A of the solution by

$$A = \alpha A_{Tr} + (1 - \alpha) A_{D+M} \qquad (4)$$

where A_{Tr} and A_{D+M} are the absorbances, at the same temperature, at the limits $\alpha = 1$ and $\alpha = 0$, respectively. $\alpha = 1$ corresponds to complete association of the triplex, i.e., the presence of Tr at $[Tr] = D_T$ plus the excess of the third strand over the duplex. $\alpha = 0$ corresponds to fully dissociated triplex.

One of the major difficulties one faces in determining α from absorbance A originates from the estimation of A_{Tr} and A_{D+M} as a function of temperature. This difficulty has been recognized for a long time (Breslauer et al., 1975), and an illustration of its effect on the recovery of thermodynamic parameters can be found in a recent paper (Longfellow et al., 1990). As other did, both A_{D+M} and A_{Tr} were extrapolated from the high- and low-temperature regions, assuming a linear absorbance versus temperature relationship for each M, D, and Tr species (upper and lower sloping baselines, respectively).

Now, let us consider a typical hysteresis cycle (Figure 2), associating a cooling curve and a heating curve obtained as described before. Let A_c, α_c, $(dT/dt)_c$, A_h, α_h, and $(dT/dt)_h$ be the absorbance, extent of association, and rate of temperature change associated with the cooling (c) and the heating (h) curves of this hysteresis cycle at the same temperature T, respectively. From the rate eq 3, it follows that

$$d\alpha_c/dT = (dT/dt)_c^{-1}[k^T_{on} M_T (1 - \alpha_c)(1 - \alpha_c/\rho) - k^T_{off}\alpha_c] \qquad (5a)$$

$$d\alpha_h/dT = (dT/dt)_h^{-1}[k^T_{on} M_T (1 - \alpha_h)(1 - \alpha_h/\rho) - k^T_{off}\alpha_h] \qquad (5b)$$

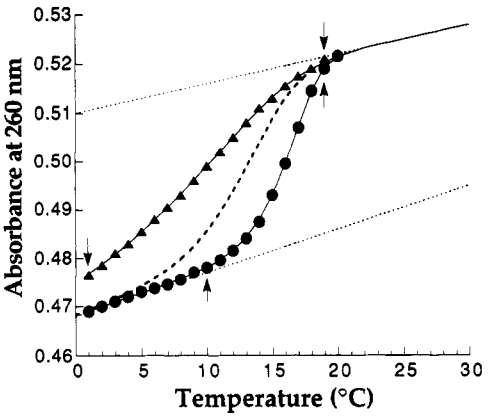

FIGURE 2: Typical hysteresis profile: duplex + 22 dG, 1/1 μM, 100 mM NaCl, and 10 mM cacodylate buffer (pH 6.8). (▲) Cooling from 20 °C at a rate of $-2.0\ 10^{-3}$ K s^{-1}; (●) heating from equilibrium at 1 °C at a rate of 2.0×10^{-3} K s^{-1}. Absorbance readings were performed every 8 min. The calculated *equilibrium* profile is represented by a dashed line. Full lines correspond to calculated absorbance changes using the Runge–Kutta algorithm (see text). Vertical arrows delimit the range of temperature where k_{on} and k_{off} are obtained with some confidence. The upper sloping baseline was obtained from independent experiments (see Figure 4).

The α's and $(d\alpha/dT)$'s are easily deduced from the hysteresis cycle by using eq 4. Hence, eqs 5a and b give us two linear relations linking the two unknowns, $k^{T}_{on}M_T$ and k^{T}_{off} (both in reciprocal seconds), which can thus be determined at any temperature T. In practice, the calculation is made at each integer value of T, with $d\alpha/dT$ at T approximated by $0.5(\alpha_{T+1} - \alpha_{T-1})$. In fact, rates of temperature change need not be constant during heating or cooling because what is needed is the instantaneous dT/dt value at each temperature, which is easily obtained from the data.

Examination of eqs 5a and b shows that coefficients of the unknowns, $k^{T}_{on}M_T$ and k^{T}_{off}, are $(1 - \alpha)(1 - \alpha/\rho)$ and α, respectively, which become increasingly small, and thus increasingly imprecise, when the corresponding curve tangentially approaches the higher (for α) and lower [for $(1 - \alpha)(1 - \alpha/\rho)$] sloping baselines. In addition, for $1 - \alpha = \epsilon$ at low temperature, $(1 - \alpha)(1 - \alpha/\rho)$ varies as ϵ^2 when $\rho = 1$, but as $(1 - 1/\rho)\epsilon$ for $\rho > 1$. This result limits the range of temperatures where the calculation gives values of $k^{T}_{on}M_T$ and k^{T}_{off} with an acceptable degree of confidence. In addition, as was well illustrated in the determination of thermodynamic parameters from thermally induced duplex–coil transitions (Breslauer et al., 1975; Cantor & Schimmel, 1980), a large portion of the accuracy in the determination of the kinetic parameters rests on the validity of the sloping baseline assumption. For the upper baseline, we have observed that, under our conditions, either the duplex or the third strands individually yield linear absorbance versus temperature plots between 0 and 30 °C. In particular, this indicates that the latter do not self-associate under these conditions. A dramatic example of self-association of single-stranded oligodeoxynucleotides and the effect it has on the recovery of thermodynamic parameters from thermally induced duplex–coil transitions has been recently published (Vesnaver & Breslauer, 1991). For the lower baseline, two controls must be exercized. First, after cooling to the lower temperature, heating must be started after equilibrium is attained. In particular, for $\rho = 1$, this time may be very long, especially when the extent of association $\alpha_{eq} = 1 - \epsilon$, with $\epsilon \rightarrow 0$, for the rate varies as ϵ^2 (this is a well-known consequence of second-order reaction kinetics). Second, the extent of association at the lower temperature must actually correspond to $\alpha_{eq} \rightarrow 1$ such that the beginning of the heating curve represents the lower sloping baseline. This condition is fulfilled if the extent of association, α_{eq}, does not increase further upon increasing the concentration of the species, since DNA concentration is the only parameter able to affect the equilibrium at constant temperature and salt conditions.

Simulation of Heating and Cooling Curves. Given the explicit analytical expressions, $k^{T}_{on}M_T = f(T)$ and $k^{T}_{off} = g(T)$, the differential eqs 5a and b do not have, to our knowledge analytical solutions. However, using the powerful fourth-order Runge–Kutta algorithm (Margenau & Murphy, 1956), numerical solutions, $\alpha(T)$, are easily obtained, starting from any pair of α and T values. This procedure has been used with two goals:

(i) From the analytical expressions $k_{on}M_T = f(T)$ and $k_{off} = g(T)$ obtained from one hysteresis cycle, it is possible to simulate any heating or cooling curve, varying the parameters at hand, i.e., dT/dt, M_T, ρ, the range of temperature scanned, etc. and compare it to the corresponding experimental curve. This method is another, more convenient, way to check that the calculated kinetic parameters used to describe the reaction under study are independent of the experimental conditions in which the melting curves have been recorded.

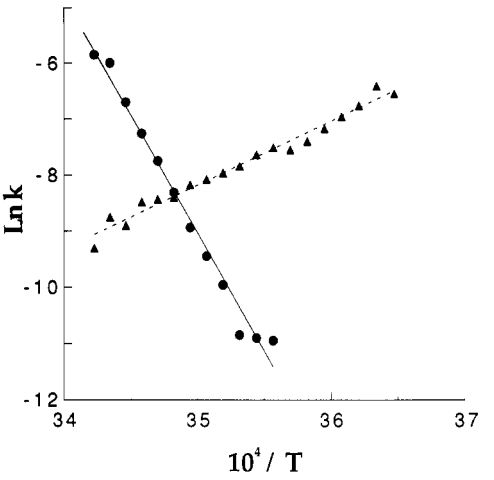

FIGURE 3: Arrhenius plot: variations of $\ln k_{on}M_T$ (▲) and $\ln k_{off}$ (●), calculated from the hysteresis profile presented in Figure 2, as a function of $1/T$.

(ii) These numerical calculations enable one to determine the extent to which small variations in experimental parameters can alter the quality of fit between the experimental and calculated curves and thus modify the calculated kinetic parameters.

RESULTS

Kinetic Parameters from Melting Curves. The values of $k^{T}_{on}M_T$ and k^{T}_{off} determined from hysteresis cycles such as that presented in Figure 2 are plotted in the form of Arrhenius plots $\ln (k^{T}_{on}M_T)$ or $\ln (k^{T}_{off})$ versus $1/T$ in Figure 3. In the temperature range delimited by the arrows in Figure 2, where these values are obtained with some confidence, straight lines are obtained with a positive slope for $k^{T}_{on}M_T$ and a negative slope for k^{T}_{off}. In other words, the activation energy, E_{on}, for the association is negative and the activation energy, E_{off}, for the dissociation is positive.

The complete hysteresis cycle was calculated by means of the Runge–Kutta algorithm and eq 4 using the following Arrhenius equations:

$$k^{T}_{on}M_T = k_{on}^{ref}M_T \exp[-(E_{on}/R)(1/T - 1/T_{ref})] \quad (6a)$$

$$k^{T}_{off} = k_{off}^{ref} \exp[-(E_{off}/R)(1/T - 1/T_{ref})] \quad (6b)$$

where $R = 1.98$ cal mol^{-1} K^{-1} $= 8.31$ J mol^{-1} K^{-1} and T_{ref} has been chosen arbitrarily at 288.15 K (15 °C). Numerical values calculated from Figure 3 are

$$k_{on}^{ref}M_T = 1.8 \times 10^{-4}\ s^{-1} \qquad k_{off}^{ref} = 4.1 \times 10^{-4}\ s^{-1}$$

$$E_{on}/R = -11\,000\ K \qquad E_{off}/R = 45\,000\ K$$

$$E_{on} = -22\ kcal\ mol^{-1} \qquad E_{off} = 90\ kcal\ mol^{-1}$$

For the cooling curve, iterative calculation started with $\alpha = 0$, $T = 303.15$ K (30 °C), and $dT/dt = -2.0 \times 10^{-3}$ K s^{-1}, while for the heating curve, it started with $\alpha = 1$, $T = 273.15$ K (0 °C), and $dT/dt = +2.0 \times 10^{-3}$ K s^{-1}. The agreement between the experimental and calculated curves is within ±0.001 absorbance unit in the midst of the transition and within ±0.002 absorbance unit toward its extremities.

As a further test of the validity of the model, we compare in Figure 4 the experimental and calculated curves obtained when, following a fast cooling from 30 to 4 °C, the sample

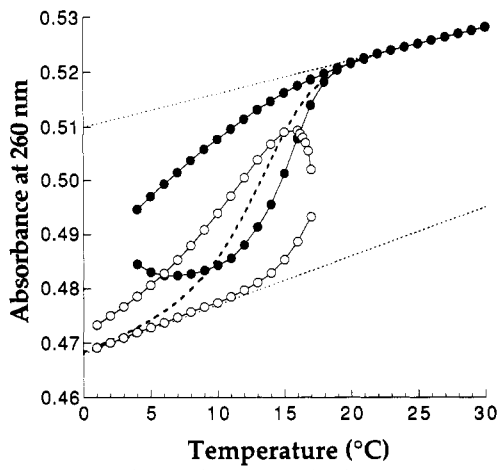

FIGURE 4: Effect of a sudden change in the temperature gradient on the heating and cooling profiles. Experimental conditions as in Figure 2. (●) A fast cooling (-7.2×10^{-3} K s^{-1}) from 30 to 5 °C is followed by a slow heating ($+1.0 \times 10^{-3}$ K s^{-1}). Absorbance was recorded every 5 min during cooling and every 15 min during heating. (○) A fast heating ($+7.2 \times 10^{-3}$ K s^{-1}) from 1 to 17 °C is followed by a slow cooling (-1.0×10^{-3} K s^{-1}). Absorbance was recorded every 5 min during heating and during cooling from 17 to 15 °C and every 15 min during cooling from 15 to 1 °C. Full lines represent the calculated absorbance changes using the Runge–Kutta algorithm (see text). The calculated equilibrium profile is represented by a dashed line (same as in Figure 2).

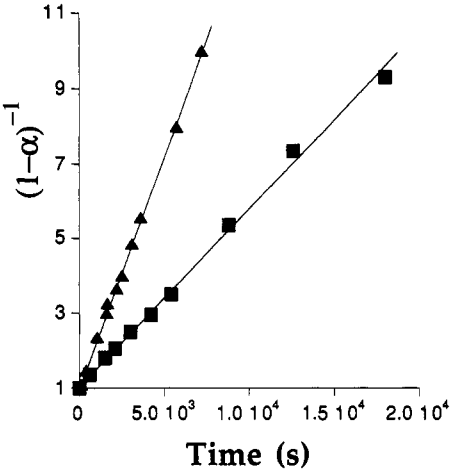

FIGURE 5: Second-order plots of $(1-\alpha)^{-1}$ as a function of time, for the isothermal association of the duplex with 22 dA in a 100 mM NaCl–10 mM cacodylate buffer (pH 6.8) at two different temperatures: (■) 8 and (▲) 2 °C. In both cases, the equilibrium position is totally shifted to the triplex form. The slopes of the straight lines are $k_{on}M_T = 1.2 \times 10^{-3}$ s^{-1} at 2 °C and 4.7×10^{-4} s^{-1} at 8 °C. Note that the reaction goes *faster* at the lowest temperature (2 °C), in good agreement with a negative association activation energy.

is heated slowly without allowing for establishment of equilibrium. The iterative calculation of the corresponding heating curve is started at $T = 5$ °C, at which point the temperature in the cell becomes well-defined. Once again, a good agreement is obtained. It can be seen in this experiment that α first continues to increase at the beginning of the heating process and then decreases upon further heating.

Starting with separated duplex and third strand ($\alpha = 0$) at high temperature, association progressively proceeds during the cooling phase. Hence, α increases with time ($d\alpha/dt > 0$). However, the temperature is decreasing with time during this phase ($dT/dt < 0$); thus $d\alpha/dT < 0$, and the bracketed expression in eq 5a is positive. Therefore, the cooling curve is above the equilibrium curve in the absorbance–temperature plot. Upon changing from cooling to heating, dT/dt becomes positive. At the beginning of the heating phase, the bracketed expression in eq 5a is positive; thus $d\alpha/dT$ is positive. Therefore, association continues to take place, with α increasing as the absorbance continues to decrease and the temperature increases. Since the dissociation becomes complete ($\alpha \rightarrow 0$) at the end of the heating phase, there is a temperature at which $d\alpha/dT = 0$. According to eq 5, this particular temperature is that at which the bracketed expression of eq 5 vanishes and the heating curve crosses the equilibrium curve. Therefore, the corresponding α value is the equilibrium value.

A similar situation is obtained when, following a fast heating of the solution equilibrated at 0 °C, the sign of the temperature change is reversed without allowing for the establishment of equilibrium and the sample is cooled slowly. Upon varying the rates of cooling and heating and the temperature at which one shifts from cooling to heating (or vice versa), the heating curve following a cooling phase (or vice versa) crosses the equilibrium curve at different temperatures. In a plot of α versus T (not shown), the tangent of the curves at these temperatures is horizontal. We prefer to report in Figure 4 the true absorbance versus temperature plots, which reflect more realistically the experimental data. In this case, the slope of the curves at these particular temperatures is obtained from eq 4, taking into account that, at these temperatures, $d\alpha/dT = 0$. Thus

$$dA/dT = \alpha(dA_{Tr}/dT) + (1-\alpha)(dA_{D+M}/dT) \quad (7)$$

where dA_{Tr}/dT and dA_{D+M}/dT are the slopes of the sloping baselines, which are assumed to be constant. The equilibrium values of T and α thus correspond to the temperature where dA/dT, α, and A simultaneously obey eqs 4 and 7.

Some isothermal kinetic measurements of association were performed in the conventional way by mixing the duplex and the third stand in a 1/1 ratio ($\rho = 1$) at temperatures below the transition midpoint, where the reaction goes to completion ($\alpha_{eq} \rightarrow 1$). Integration of the rate law, eq 3, with $k^T_{off}\alpha \ll k^T_{on}M_T(1-\alpha)^2$ leads to the second-order expression, $(1-\alpha)^{-1} = 1 + k^T_{on}M_T t$, where α, as previously defined, is the fraction of duplex engaged in the triplex. An example is shown in Figure 5. Linear second-order plots were obtained to at least 90% completion, and the corresponding values of $k^T_{on}M_T$ are in good agreement with the values calculated from the hysteresis curves. As expected from the integrated isothermal kinetic law obtained from eq 3, the reaction runs faster at temperatures within the transition because the rate of association does not vanish at equilibrium ($\alpha_{eq} < 1$), in spite of the fact that k^T_{on} decreases and k^T_{off} increases as the temperature increases.

From the values of $k^T_{on}M_T$ and k^T_{off}, a straightforward calculation leads to the equilibrium values α_{eq} by means of the following equation:

$$d\alpha_{eq}/dt = k^T_{on}M_T(1-\alpha_{eq})(1-\alpha_{eq}/\rho) - k^T_{off}\alpha_{eq} \equiv 0 \quad (8)$$

The calculated equilibrium curve is presented as dashed lines in Figures 2 and 4. The standard molar enthalpy change for the formation of the triplex from the duplex and the third strand is simply

$$\Delta H^\circ = E_{on} - E_{off}$$

The standard molar entropy change ΔS° can be determined from the relation

$$\Delta H^\circ - T_m\Delta S^\circ = -RT_m \ln K_{eq}(T_m)$$

where $K_{eq}(T_M) = (1 - {}^1/_2\rho)^{-1}M_T^{-1} = 2M_T^{-1}$ for $\rho = 1$ and T_m is the temperature where $\alpha = 0.5$.

Table I: Association Kinetic Parameters k_{on} (15 °C) and E_{on} in 10 mM Cacodylate (pH 6.8) as a Function of NaCl Concentration[a]

	[NaCl] (mM)				
	20	40	100	200	300
k_{on} (15 °C)[b] (M^{-1} s^{-1})	13	48	180	300	900
E_{on}[c] (kcal mol^{-1})	−28	−26	−22	−20	−16

[a] These values are independent of the nature of nucleotide N in the third strand. [b] ±20%. [c] ±10%.

Table II: Dissociation Kinetic Parameters k_{off} (15 °C) and E_{off} in 10 mM Cacodylate (pH 6.8) as a Function of Nucleotide N in the Third Strand[a]

	nucleotide N			
	T	A	G	C
k_{off} (15 °C)[b] (s^{-1})	1.5 ± 10^{-6}	7.9×10^{-5}	4.1×10^{-4}	2.0×10^{-3}
E_{off}[c] (kcal mol^{-1})	90	90	90	90

[a] These values are independent of the NaCl concentration. [b] ±20%. [c] ±10%.

Effects of Mismatches and NaCl Concentration. The association of the four 22-dN third strands with the same target duplex was studied in the same detailed manner as described above at NaCl concentrations ranging from 20 to 300 mM (Tables I and II). In all cases, the general pattern was the same: Arrhenius plots such as that presented in Figure 3 are linear, with a negative activation energy, E_{on}, for the association. Thus, triplex formation from duplex and third strand behaved similarly to the well-studied duplex formation from complementary single strands (Craig et al., 1971; Pörschke & Eigen, 1971; Cantor & Schimmel, 1980), though it occurred at a much slower rate. The negative value for E_{on} indicates that the association is not an elementary step whose activation energy would be small and positive, but is rather a more complex process, which will be further discussed below. Nevertheless, the kinetic data fulfill the predictions of the two-state model in the sense that no breaks or curvatures are observed in the Arrhenius plots, as would possibly occur if intermediate states with partial base pairing were populated during the reaction.

Taking into account the overall precision of the determination of the kinetic parameters (±10% for E_{on} and E_{off} and ±20% for k_{on} and k_{off} at a chosen reference temperature), the general trends observed upon varying the sequence of the third strand (N = T, A, C, G) and the NaCl concentration are the following (see Tables I and II and Figure 6):

(i) Up to a 5-fold increase of M_T shifted both the cooling and the heating curves toward higher temperatures, the latter to a lesser extent than the former, but the calculated k^T_{on} and k^T_{off} values remained unchanged. Thus, from a kinetic point of view, the association reaction is second order while the dissociation reaction is first order.

(ii) Arrhenius plots for association were independent of the nature of nucleotide N in the third strand and depended only on NaCl concentration. The rate constant, k_{on}^{ref}, strongly decreased and E_{on} became slightly but measurably more negative when the NaCl concentration was decreased.

(iii) Arrhenius plots for dissociation were independent of NaCl concentration. The rate constant, k_{off}^{ref}, strongly decreased in the order C > G > A ≫ T, while E_{off} remained rather independent of N. (T in the third strand corresponds to a perfect match in the triplex sequence.)

(iv) $\Delta H°$ ($=E_{on} - E_{off}$) decreased slightly when the NaCl concentration was increased. However, the effects are small and fall within the experimental error.

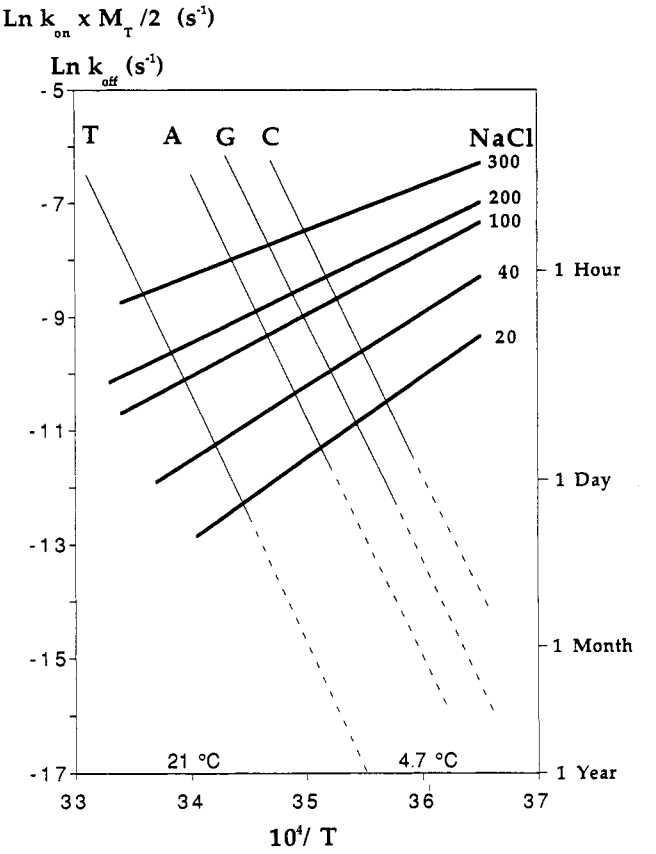

FIGURE 6: Arrhenius plots of $k_{on}M_T/2$ (with M_T = 1 μM) and k_{off}, both in reciprocal seconds. NaCl concentrations, in millimolar, are reported on the association lines ($k_{on}M_T/2$, in bold-face type). The nature of the nucleotide N in the third strand is reported on the dissociation (k_{off}) lines. For k_{off} profiles, the full lines correspond to the range of temperatures where k_{off} was experimentally obtained, and dashed lines to extrapolations. Intersections between two lines give the corresponding T_m at 1 μM.

The values of the different kinetic parameters are reported in Tables I and II. In a perhaps more illustrative way, the Arrhenius plots of $k^T_{on}M_T/2$ with M_T = 1 μM and k^T_{off} are given in Figure 6. The intersections of the straight lines give the T_m values at that concentration. On the right ordinate are reported some selected values of the times corresponding to the left ordinate scale. This representation emphasizes the considerable inertness, from the kinetic point of view, that these triplex structures can experience at low temperatures.

Effect of $MgCl_2$ Addition. Addition of increasing amounts of $MgCl_2$ in the presence of 20 mM NaCl dramatically increased the reaction rate. Both the heating and cooling curves were shifted toward higher temperatures, and the difference between heating and cooling progressively decreased when [$MgCl_2$] was increased. With a rate $dT/dt = \pm 3.3 \pm 10^{-3}$ K s^{-1}, the difference in midpoint temperatures became less than 0.2 °C for $MgCl_2$ concentrations higher than 40 mM. In other words, the cooling and heating curves tended to merge, thus leading to a reversible melting profile. Van't Hoff plots of ln K_{eq} versus $1/T$ were linear, consistent with the prediction of a two-state model. In going from 0 to 40 mM $MgCl_2$, $\Delta H°$ remained unchanged (≈−110 kcal/mol) but the T_m increased from 7 to 23 °C (22 dC), 9 to 26.5 °C (22 dG), 11.5 to 28 °C (22 dA), and 17 to 35 °C (22 dT). This stabilization amounts to a $\Delta(\Delta G°) \approx -6.5$ kcal/mol, which corresponds to a ≈40 000-fold increase of the equilibrium constant K_{eq}.

DISCUSSION

The formation of triplex structures by association of a homopurine–homopyrimidine duplex with a third homopyrimidine single strand resembles in many aspects the formation of a duplex by association of two complementary single strands. Insights into the mechanism of these reactions are provided by the characteristic features of their kinetics. For example, Pörschke and Eigen (1971), in their pioneering study of the association of A_n with U_n (n = 8–18) already obtained negative "apparent" activation energies for strand association and interpreted their results within the now so-called nucleation-zipping model. For their system, the time scale for the reactions was in the range of millisecond to second; thus the appropriate techniques were T-jump relaxation and stopped-flow spectroscopy. However, they noticed that a relaxation time longer by a factor of 100 was observed, corresponding to the equilibration of triple helices oligo(A)·2oligo(U). In the following paper, Craig et al. (1971) presented a detailed kinetic scheme which could adequately describe the helix growth and opening processes and compared it to their experimental work on the A_nU_n self-complementary oligonucleotides.

These authors concluded that double-helix formation begins with two or three bases pairing and unpairing in rapid but unfavorable equilibrium. Then, when the critical intermediate adds one more base pair, a helix nucleus is formed, which zips up to form the fully bonded helix more rapidly than it dissociates to single strands. The rate of the overall association, namely, the rate of the rate-determining step of the reaction, is simply the concentration of the critical intermediate times the first-order rate constant for adding one base pair. It follows that the rate equation for the association is second order in single strands because the concentration of the critical intermediate depends on the square of the strand concentration (for self-complementary species) or on the product of the strand concentrations (for non-self-complementary species).

More recently, Anshelevich et al. (1984), using a somewhat different approach (the simplified version of their model ranking with the classical "gambler ruin" problem of probability theory), focused on the theoretical determination of the mean time required for complete separation of complementary chains of duplexes, which is essentially the lifetime of the double helix. Their result for oligonucleotides [eq 32 of Anshelevich et al. (1984)] coincides with the corresponding equation obtained by Craig et al. (1971).

Following both approaches of the kinetics of association–dissociation, together with the equilibrium formulation of the transition developed in particular by Applequist and Damle (1965) and Zimm (1960), the nucleation-zipping model as it applies to triplexes can be briefly summarized as follows:

(i) The equilibrium constant $K = k_{on}/k_{off} = \beta s^n$, where β is the equilibrium constant for nucleation of the triplex (equilibrium constant for the formation of the first base triplet), s, the dimensionless chain growth parameter, is the ratio, k_f/k_b, of the first-order rate constants for the formation (f) and breakage (b) of the base triplet at the end of a triplex segment (these rate constants are assumed to be independent of the sequence in this simplifying first approximation), and n is the total number of base triplets being formed.

(ii) The second-order association rate constants $k_{on} = 2(n - \nu)\beta s^\nu k_f$, where ν is the number of base triplets in the nucleus, which is in rapid equilibrium with the separated duplex + third strand, and from which zipping leads to the fast complete association. Hence, the first-order dissociation rate constant, k_{off}, is given by

$$k_{off} = k_{on}/K = 2(n - \nu)s^{\nu-n}k_f$$

(iii) Consequently, the activation energy, $E_{on} = d \ln k_{on}/d(1/T)$, is the sum of one kinetic activation energy, E_{k_f}, and $\nu + 1$ reaction enthalpies for base triplet formation reactions, $\Delta H_\beta + \nu\Delta H_s$:

$$E_{on} = E_{k_f} + \Delta H_\beta + \nu\Delta H_s$$

The first term is small and positive but the enthalpies are negative, such that E_{on} becomes negative, its magnitude increasing with ν. The activation energy for dissociation, $E_{off} = E_{k_f} - (n - \nu)\Delta H_s$, is always largely positive.

We shall discuss below the influence of three experimental parameters, temperature, salt concentration, and mismatch at the center of the third strand, on the rate constants k_{on} and k_{off} and hence, on their ratio $K = k_{on}/k_{off}$, via their expected influence on the model's parameters ν, β, s, and k_f, referring to what has been found in the duplex case and explained in detail by Craig et al. (1971) and Pörschke and Eigen (1971).

(1) Temperature Effects. As noted above, the negative values we have obtained for E_{on} are a strong argument in favor of the nucleation-zipping model. From the expressions giving E_{on} and $\Delta H°$ (see above), it is possible to obtain an estimation of the number of base triplets in the nucleus. As has been found in the duplex case, we assume, to a first approximation, that β and k_f are temperature independent (more precisely, that $E_{k_f} + \Delta H_\beta \sim 0$, the first one being small and positive, the second small and negative), such that the temperature dependence of the kinetic parameters k_{on} and k_{off}—and of the equilibrium constant K—rests only upon the temperature dependence of the growing chain factor s. It follows that $E_{on} \sim \nu\Delta H_s$ and $\Delta H° \sim n\Delta H_s$. Hence, $\nu = nE_{on}/\Delta H°$.

We have shown that E_{on} is dependent on the ionic strength and independent of the mismatch in the third strand and that E_{off} is independent of both factors. It follows that $\nu = 22 \times 16/106 = 3.3$ at 300 mM NaCl and $\nu = 22 \times 28/118 = 5.2$ at 20 mM NaCl. Of course, ν must be an integer value, so it increases roughly from 3 to 5 base triplets when the NaCl concentration is decreased from 300 to 20 mM.

Our $\Delta H°$ value of about –112 kcal mol^{-1} at 100 mM NaCl, for 22 (or 21) base triplets gives a mean value of –5 kcal mol^{-1} of base triplet, which is significantly lower than that of the mean enthalpy change per Watson–Crick base pair in duplexes (Breslauer et al., 1986). Other recently reported mean $\Delta H°$ values (in kilocalories per mole of base triplet) are either comparable [–5.8 (Xodo et al., 1990)], slightly higher [–6.6 (Manzini et al., 1990)], or much lower [–2.3 and –4.2 (Pilch et al., 1990a)]. These variations may arise from differences in the methods and models used for analysis, pH, ionic strength, and/or base composition. A more intriguing case has been recently reported by Plum et al. (1990). Using both differential scanning calorimetry (DSC) and UV spectroscopy, they obtained a very low calorimetric (model independent) mean value of –2.0 kcal mol^{-1} of base triplet, which is about 3 times lower than their van't Hoff (model dependent) mean value derived from both the UV melting curves and DSC shape analysis.

Concerning the chain growth factor s, its value is not very different from that of a duplex of comparable length. For example, at the T_m of any bimolecular–unimolecular transition one always has $K = \beta s^n = 2/M_T$. Since n is large, differences in β values between the duplex and the triplex cases do not

greatly affect s values at the T_m. As an example, with $\beta = 10^{-3}$ (10^{-6}) M^{-1}, $s = 2.6$ (3.6) at the T_m of a micromolar solution of a 22 mer ($n = 22$). For a 14 mer such as A_7U_7, $s = 4.6$ (7.6) (Craig et al., 1971). Also, the temperature dependence of s is governed by the ΔH_s values, which are not very different. With $\Delta H_s \sim -5$ kcal mol^{-1} of base triplet, the corresponding values for $n = 22$, at a temperature 10 °C below the T_m, are approximately $s = 3.5$ (4.9). Since the T_m of the duplex is higher than that of the triplex, the s value of the duplex is higher than that of the triplex at any temperature.

(*2*) *Salt Effects.* Our finding that k_{on} strongly decreases upon decreasing ionic strength whereas k_{off} is independent of NaCl concentration is also consistent with the observations in the case of duplex DNA [Braulin and Bloomfield (1991) and references therein]. Hence, the dependence of the kinetics of association on ionic strength is almost completely determined by the ionic strength dependence of β (Anshelevich et al., 1984), which appears in k_{on}, but not in k_{off}. A considerable decrease in β (up to 5 orders of magnitude on decreasing NaCl concentration from 1 to 10^{-2} M) has been reported (Blake & Fresco, 1966; Anshelevich et al., 1984) from polymeric DNA renaturation kinetics. At high ionic strength (≈0.15–0.25 M), $\beta \sim 10^{-3}$ M^{-1} for the self-complementary A_5U_5 oligomer (Craig et al., 1971) and for $A_n{\cdot}U_n$ (Pörschke & Eigen, 1971). For the self-complementary octamer $G_2A_2T_2C_2$, k_{on} varies as $[Na^+]^{1.4}$ between 0.046 and 0.267 M whereas k_{off} decreases from 4.6×10^3 to 1.8×10^3 s^{-1} (Braulin & Bloomfield, 1991). In our case, k_{on} varies as $[Na^+]^{1.5}$ between 20 and 300 mM NaCl (see Table I).

We do not know the magnitude of β in the triplex case, but it can be inferred that β would be even lower than that for duplex nucleation. In both cases, nucleation implies a proper alignment of the strands in order to successfully achieve the first base pairing leading to the nucleus and, then, to the full helix. Electrostatic repulsion between the negatively charged phosphates is the determining factor in the pairing of the first bases before they become stabilized by stacking interactions. These electrostatic repulsions may be more important in the triplex than in the duplex because the third strand has to come into contact with the duplex that exhibits twice the charge density of a single strand. However, as explained in detail by Craig et al. (1971), nucleation can proceed anywhere in the sequence provided the bases are in the proper alignment. Hence, the possible favorable participation of positively charged protonated cytosines in some nucleation steps must be taken into account. In addition, the two partners have to adopt a favorable configuration and wrap around each other in order to achieve base pairing. This may be easier in the duplex case, where the two single strands are relatively flexible in solution, rather than in the triplex case, where the single strand has to coil around the major groove of the more rigid duplex. In addition, the duplex must undergo a conformational change when the triplex forms (Arnott & Selsing, 1974). This change may also explain why the number of base triplets involved in nucleation (3–5) is significantly higher than the values obtained in the duplex case (2–3).

In the duplex case, separate estimations of β and s have been obtained. For example, from the variations of T_m as a function of length, n, it was possible to derive the values of k_f from the association kinetics. Such estimations ranged between 10^6 and 10^8 s^{-1} and thus between 10^5 and 10^7 s^{-1} for $k_b = k_f/s$. The k_{on} values we obtained are roughly 10^3–10^4 times smaller than those of duplex association and may be attributed to a corresponding lower β value in the triplex case, although a decrease of k_f and k_b in the triplex relative to the duplex case cannot be excluded. Furthermore, k_{off} values, with E_{off} of about 90 kcal mol^{-1}, strongly decrease when the temperature decreases (Figure 6), and dissociation may become very slow. As stressed by Pörschke and Eigen (1971), "the rates of dissociation are quite slow, although the elementary times of opening and closing of individual base (triplets) are very short".

Comparison of the k_{off} values for triplex and duplex dissociation is difficult, because E_{off} for a duplex of the same length is much higher. As an element of comparison, the T_m for the dissociation of the 22dR·22dY duplex at 1 μM strand concentration, pH 5.8–7.2 and 100 mM NaCl, is about 50 °C (data not shown). Assuming a k_{on} value of about 10^6 M^{-1} s^{-1}, a k_{off} value of about 0.5 s^{-1} may be calculated at the T_m for the duplex. Extrapolation of the van't Hoff plot of k_{off} for the triplex where $N = T$ yields a $k_{off} \approx 20$ s^{-1} at that temperature. It therefore seems that the difference between the k_{off} values of the duplex and triplex is less important than the difference between their k_{on} values.

Finally, for each of the four third strands studied, the destabilization, in the thermodynamical sense, of the triplex when the NaCl concentration is decreased originates almost completely from the decrease of the second-order rate constant of association k_{on}, via a decrease of the nucleation parameter β.

(*3*) *Effect of $MgCl_2$ Addition.* Divalent cations such as Mg^{2+} are known to strongly stabilize triplex structures in the absence or presence of low concentrations of monovalent cations. The 40 000-fold increase of the equilibrium constant K_{eq} in going from 0 to 40 mM $MgCl_2$ in the presence of 20 mM NaCl arises, in a large part, from an increase of the association rate constant k_{on}, probably via an increase of the nucleation parameter β. The minimal increase in k_{on} may be estimated as follows: When the shift, ΔT, between the heating and the cooling curves is low, its value around the T_m may be derived from eq 5 and is given by

$$\Delta T \approx (dT/dt)(k_{on}M_T)^{-1} \approx {}^1/_2(dT/dt)(k_{off})^{-1}$$

Assuming $\Delta T < 0.2$ K; $dT/dt = 3.3 \times 10^{-3}$ K s^{-1}, and $M_T = 1$ μM, $k_{on}M_T > 2 \times 10^{-2}$ s^{-1}. Hence $k_{on} > 2 \times 10^4$ M^{-1} s^{-1}, which is about 1500 times the 13 M^{-1} s^{-1} value obtained in the absence of $MgCl_2$.

(*4*) *Effect of a Point Mutation in the Third Strand.* We have previously shown that a single mismatched triplet can strongly destabilize a triplex structure (Mergny et al., 1991). The destabilization, in the thermodynamical sense, of the triplex upon going from 22 dT to 22 dC originates mainly from the increase of the dissociation rate constant, k_{off}. Since the value of E_{off} is constant, this increase is temperature independent. In addition, it does not depend on NaCl concentration, all this within experimental uncertainty. The triplex formed by 22 dT contains only canonical base triplets, either T×A·T or CH^+×G·C. The three other third strands present a mismatch in the center of the triplex structure, and the destabilization depends on the nature of the mismatched base in the order C < G < A. From the results reported in Table II, the ratio $k_{off}(22\ dC)/k_{off}(22\ dT)$ is about 1.4×10^3, which corresponds to a difference in the dissociation activation free energy $\Delta G^{\ddagger}(22\ dT) - \Delta G^{\ddagger}(22\ dC) = RT \ln (k_{off}(22\ dC)/k_{off}(22\ dT) \approx 4.2$ kcal mol^{-1}. Since k_{on} has the same value for the four third strands, the difference in the standard free energy, $\Delta G°$, of the reaction is of the same order as that of $\Delta G^{\ddagger}$. Whether these differences are of enthalpic and/or entropic origins cannot be determined from our results because E_{off} and $\Delta H°$ are determined with an error of ±10%. The

standard free energy $\Delta G°$ ($=\Delta H° - T\Delta S°$) of any bimolecular–unimolecular reaction is given by $\Delta G° = -RT \ln K_{eq}$, with $K_{eq} = \alpha/(1 - \alpha)^2 C_T$. The magnitude of $\Delta G°$ at a T_m ($\alpha = 0.5$) around 300 K and $C_T = 10^{-6}$ M is approximately −8.7 kcal mol^{-1}. A 100-fold increase (or decrease) of K_{eq} via increase (or decrease) of α upon decreasing (or increasing) the temperature from the T_m at constant C_T changes $\Delta G°$ by only $\pm\sim$2.8 kcal mol^{-1}. Actually, the most reliable thermodynamic parameter derived from optical melting is $\Delta G°$ at the T_m (Longfellow et al., 1990) and within the transition, because it is directly determined from α and C_T. In our case and in the case of all duplex- or triplex-forming reactions between oligonucleotides of similar length, the rather low values of $\Delta G°$ result from the difference between the two much higher enthalpic ($\Delta H°$) and entropic ($-T\Delta S°$) contributions, which are of the same order of magnitude (e.g., $\Delta H° \sim -112$ kcal mol^{-1}, hence $T\Delta S° \sim -103$ kcal mol^{-1} at the T_m for $C_T = 10^{-6}$ M).

For a given third strand, the approximate $\Delta H°$ and $\Delta S°$ values we obtained do not prevent us from estimating K_{eq} and thus the population of the different species actually present in solution at any temperature within a limited range outside the temperature range of the transition. However, assignment of the $\Delta\Delta G° \sim 4$ kcal mol^{-1} in changing 22 dT to 22 dC to a corresponding change in $\Delta H°$ and/or $\Delta S°$ would require determination of these thermodynamic parameters with much better accuracy. Examination of both old and recent studies on the thermodynamics of fast duplex formation in the oligoribo and the oligodeoxyribo series with or without mismatches, bulges, or loops (Breslauer et al., 1986; Li et al., 1991; Longfellow et al., 1990; Petersheim & Turner, 1983) reveals that this determination is a difficult task that is beyond the scope of our study, which dealt mainly with the general kinetic aspects of triplex-forming reactions.

The simplified nucleation-zipping model described above does not take into account the probable sequence-dependence of β, k_f, and k_b, which are given as mean values. In our system, the sequences of the third strands are the same except for the central base N. That only k_{off} is changed in going from 22 dT to 22 dC can be explained as follows. Obviously, introducing a break in the center of the triplex should considerably perturb the rate parameters k_f and k_b at the mismatch itself and in its immediate vicinity, but is not expected to affect their values outside the mismatched region. Thus, nucleation events in this region should be less favorable, while all those occurring outside this region should be unaffected. Since the apparent second-order rate constant of the association depends mainly on those s values which are unaffected by the mismatch and does not depend on the rate of zipping, if higher than that of nucleation, k_{on} remains approximately independent of the presence of the mismatch. Conversely, as explained, for example, by Pörschke and Eigen (1971), dissociation of the triplex has to overcome an activation barrier (on the average 90/22 = 4.1 kcal mol^{-1}), triplet after triplet from the extremities, until there remains only $\nu - 1$ triplets beyond which no activation barrier is left for complete dissociation. In doing so, dissociation passes through the mismatched region where the activation barrier is abolished, thus accelerating the process. This is an oversimplified view which should be completed by further experimental results.

CONCLUSION

In conclusion, the kinetic measurements reported in the present study demonstrate that triplex formation from a duplex and a single strand is a slow process as compared to duplex formation from single strands. The association rate constants at 300 mM NaCl differ by approximately 3 orders of magnitude. The activation energy for triplex formation is negative and corresponds to the formation of three to five base triplets as a required nucleus before the full triplex forms. This nucleation phase is the rate-limiting step in the association reaction. Mismatches in the center of the triplex do not affect the association rate but increase the dissociation rate of the triplex. In the absence of a multivalent cation, a decrease in NaCl concentration has no effect on triplex dissociation but strongly decreases the rate constant of association. Consequently, triplexes are only marginaly stable at 20 mM NaCl. A small degree of deviation from the two-state assumption underlying this work should not alter the qualitative nature of our conclusion about the effect of NaCl concentration and mismatches on the kinetics of triplex-forming reactions. Multivalent cations (Mg^{2+}, spermine 4+) are known to stabilize triplex structures. Increasing NaCl concentrations lowers the extent of binding by multivalent cations and may, therefore, lead to opposite effects on triplex stability as compared to NaCl addition in the absence of multivalent cations. Kinetic phenomena should be taken into account when triple helix-forming oligonucleotides are used to compete with sequence-specific DNA-binding proteins which have much faster association kinetics. Experiments in cell cultures have shown that oligonucleotides can indeed compete with transcription activators (Grigoriev et al., 1992; Postel et al., 1991). However, the time dependence of transcription inhibition remains to be explored.

REFERENCES

Anshelevich, V. V., Vologodskii, A. V., Lukashin, A. V., & Frank-Kamenetskii, M. D. (1984) *Biopolymers 23*, 39–58.

Applequist, J., & Damle, V. (1965) *J. Am. Chem. Soc. 87*, 1450–1468.

Arnott, S., & Selsing, E. (1974) *J. Mol. Biol. 88*, 509–521.

Blake, R. D., & Fresco, J. R. (1966) *J. Mol. Biol. 19*, 145–160.

Blake, R. D., Massoulié, J., & Fresco, J. R. (1967) *J. Mol. Biol. 30*, 291–308.

Blake, R. D., Klotz, L. C., & Fresco, J. R. (1968) *J. Am. Chem. Soc. 90*, 3556–3562.

Braulin, W. H., & Bloomfield, V. A. (1991) *Biochemistry 30*, 754–758.

Breslauer, K. J., Sturtevan, J. M., & Tinoco, I., Jr. (1975) *J. Mol. Biol. 99*, 549–565.

Breslauer, K. J., Franck, R., Blöcker, H., & Marky, L. A. (1986) *Proc. Natl. Acad. Sci. U.S.A. 83*, 3746–3750.

Cantor, C. R., & Warshaw, M. M. (1970) *Biopolymers 9*, 1059–1077.

Cantor, C. R., & Schimmel, P. R. (1980) *Biophysical Chemistry*, Part III, W. H. Freeman and Co., San Francisco.

Craig, M. E., Crothers, D. M., & Doty, P. (1971) *J. Mol. Biol. 62*, 383–401.

De los Santos, C., Rosen, M., & Patel, D. (1989) *Biochemistry 28*, 7282–7289.

Felsenfeld, G., Davies, D. R., & Rich, A. (1957) *J. Am. Chem. Soc. 79*, 2023.

Grigoriev, M., Praseuth, D., Robin, P., Hemar, A., Saison-Behmoaras, T., Dautry-Varsat, A., Thuong, N. T., Hélène, C., & Harel-Bellan, A. (1992) *J. Biol. Chem. 267*, 3389–3395.

Le Doan, T., Perrouault, L., Praseuth, D., Habhoub, N., Decout, J.-L., Thuong, N. T., Lhomme, J., & Hélène, C. (1987) *Nucleic Acids Res. 15*, 7749–7760.

Li, Y., Zon, G., & Wilson, W. D. (1991) *Biochemistry 30*, 7566–7572.

Longfellow, C. E., Kierzek, R., & Turner, D. H. (1990) *Biochemistry 29*, 278–285.

Lyamichev, V. L., Mirkin, S. M., Frank-Kamenetskii, M. D., & Cantor, C. R. (1988) *Nucleic Acids Res. 16*, 2165–2178.
Maher, L. J., III, Dervan, P. B., & Wold, B. J. (1990) *Biochemistry 29*, 8820–8826.
Manzini, G., Xodo, L. E., Gasparotto, D., Quadrifoglio, F., van der Marel, G. A., & van Boom, J. H. (1990) *J. Mol. Biol. 213*, 833–843.
Marck, C., & Thiele, D. (1978) *Nucleic Acids Res. 5*, 1017–1028.
Margenau, H., & Murphy, G. M. D. (1956) *The Mathematics of Physics and Chemistry*, Van Nostrand Cie, New York.
Marky, L. A., & Breslauer, K. J. (1987) *Biopolymers 26*, 1601–1620.
Mergny, J. L., Sun, J. S., Rougée, M., Montenay-Garestier, T., Barcelo, F., Chomilier, J., & Hélène, C. (1991) *Biochemistry 30*, 9791–9798.
Morgan, A. R., & Wells, R. D. (1968) *J. Mol. Biol. 37*, 63–80.
Moser, H. E., & Dervan, P. B. (1987) *Science 238*, 645–650.
Petersheim, M., & Turner, D. (1983) *Biochemistry 22*, 256–263, 264–268, 269–277.
Pilch, D. S., Brousseau, R., & Shafer, R. H. (1990a) *Nucleic Acids Res. 18*, 5743–5750.
Pilch, D. S., Levenson, C., & Shafer, R. H. (1990b) *Proc. Natl. Acad. Sci. U.S.A. 87*, 1942–1946.
Plum, G. E., Park, Y. W., Singleton, S. F., Dervan, P. B., & Breslauer, K. J. (1990) *Proc. Natl. Acad. Sci. U.S.A. 87*, 9436–9440.
Pörschke, D., & Eigen, M. (1971) *J. Mol. Biol. 30*, 291–308.
Postel, E. H., Flint, S. J., Kessler, D. J., & Hogan, M. E. (1991) *Proc. Natl. Acad. Sci. U.S.A. 88*, 8227–8231.
Rajagopal, P., & Feigon, J. (1989) *Biochemistry 28*, 7859–7870.
Sun, J. S., François, J. C., Montenay-Garestier, T., Saison-Behmoaras, T., Roig, V., Chassignol, M., Thuong, N. T., & Hélène, C. (1989) *Proc. Natl. Acad. Sci. U.S.A. 86*, 9198–9202.
Vesnaver, G., & Breslauer, K. J. (1991) *Proc. Natl. Acad. Sci. U.S.A. 88*, 3569–3573.
Xodo, L. E., Manzini, G., & Quadrifoglio, F. (1990) *Nucleic Acids Res. 18*, 3557–3564.
Zimm, B. H. (1960) *J. Chem. Phys. 33*, 1349.